

Arrayed, Piezoelectrically-Actuated Mirrors and Gratings for Spectrometer

Shih-Jui Chen¹, Derrick Chi, Joe Lo, and Eun Sok Kim

Department of Electrical Engineering – Electrophysics,
University of Southern California, Los Angeles, CA 90089, USA

ABSTRACT

This paper describes a technology for a compact spectrometer based on a 2D piezoelectric mirror and/or grating array. The piezoelectric mirror/grating array is composed of angularly movable, 2-D array of micromirrors/microgratings that is supported on piezoelectric cantilevers, and can be driven piezoelectrically with controllable tilt angle in both upward and downward directions. A large reflecting/diffractive surface is obtained through a combination of the small-sized mirrors/gratings that are surface-micromachined without fabrication difficulties associated with a large size mirror/grating.

Keywords: MEMS spectrometer, piezoelectric, actuated micromirror, grating, mirror array

1 INTRODUCTION

Optical spectrometers consisting of a light source, a wavelength-separation device and a light detector are built for applications to lifetime fluorescence, transmission/absorbance of the materials, Raman spectroscopy, and color analysis in medical, optical, and biological research. Many prototype miniature spectrometers using MEMS techniques have been developed [1-7] to shrink the size and lower the manufacturing cost of the spectrometer, usually at a reduced performance level. Thus, balancing the size and performance is an important design tradeoff in designing current generation of microspectrometers.

This paper describes a newly fabricated and tested piezoelectric mirror/grating array composed of angularly movable, 2-D array of micromirrors/microgratings that is supported on a large number of piezoelectric cantilevers. Since the mirror/grating is formed through an array of small-sized mirrors/gratings, a large optical throughput is obtained without fabrication difficulties associated with a large size mirror/grating. An array of the small-sized mirrors/gratings was surface-micromachined, and is ready to be integrated with additional fiber array, microlens array and detector array. Incorporating all such components as shown in Figure 1 will result in a compact spectrometer, which can be used in endoscopic treatment, microsurgery, etc.

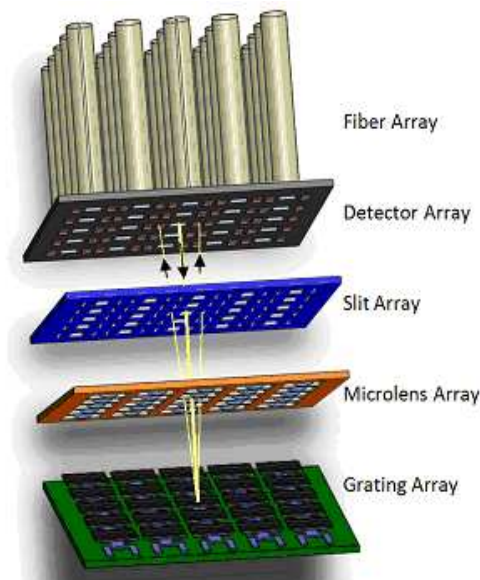


Figure 1: Schematic of a microspectrometer based on a piezoelectrically actuated diffraction grating array.

2 DESIGN AND FABRICATION

Plane mirrors are the most commonly used optical components, and there are many applications that would benefit from a large, flat mirror with a high reflectivity that is surface-micromachined. However, a large, surface-machined mirror is usually warped, and diminishes optical throughput. As a substitute for a large contiguous mirror, we have fabricated a 2-D mirror array on piezoelectric cantilevers that can tilt the mirror array linearly over a wide range in both upward and downward directions.

2.1 Process Flow

Piezoelectric cantilevers are composed of low-stress LPCVD silicon nitride, Al, piezoelectric ZnO, PECVD silicon nitride and Al alloy (from bottom to top), and were fabricated according to the steps shown in Fig. 2(a), as we adjusted the SiO₂ layer thickness to compensate the residual stress.

First, we deposited 0.4 μm thick low stress silicon nitride and thermal oxide, followed by 0.1 μm thick Al

¹ Shih-Jui Chen, Department of EE–Electrophysics, University of Southern California, 3737 Watt Way, PHE510, Los Angeles, CA 90089-0271, U.S.A., Tel: 1-213-821-1611, Fax: 1-213-740-8677, Email: shihjuic@usc.edu.

electrode deposition (by e-beam evaporation) and patterning for the bottom electrode of the piezoelectric actuator. Then, 0.45 μm thick ZnO was deposited by RF sputtering at 300 $^{\circ}\text{C}$, followed by Plasma Enhanced Chemical Vapor Deposition of 0.1 μm thick silicon nitride at 275 $^{\circ}\text{C}$. After 0.1 μm thick top Al electrode was deposited and patterned, the ZnO and SiN_x were patterned by wet acid and CF₄ reactive ion etching (RIE), respectively.

Then a thick photoresist (used as sacrificial layer) was spin-coated and patterned (Fig. 2(b)), followed by sputter-deposition and patterning of aluminum alloy to form the mirror structure (Fig. 2(c)). Photoresist stripper was used to remove the sacrificial layer. Finally, the mirror structure was released through XeF₂ etching of the silicon substrate (Fig. 2(d)).

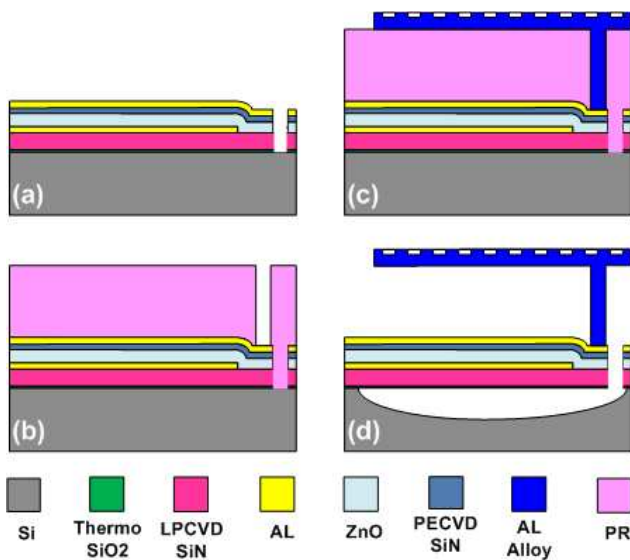


Figure 2: Brief process flow of the mirror/grating array.

2.2 Fabricated Device

The fabricated mirror array showed some initial warping due to a large compressive stress in the ZnO film (Fig. 3). The as-fabricated warping angle of a few degree was, though, much better than the warping angle of several tens of degree for a large contiguous mirror.

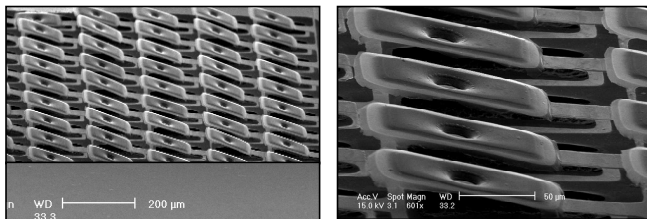


Figure 3: SEM photos of a fabricated mirror array

Furthermore, we fabricated a piezoelectric grating array (Fig. 4), which can be integrated to form a wavelength-

selectable, compact 2D spectrometer such as the one shown in Fig. 1.

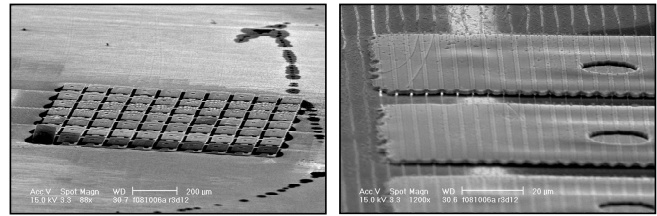


Figure 4: SEM photos of a fabricated grating array.

The mirror/grating array consists of 70 individual small mirrors/gratings (arranged as 7x10). The mirror/grating area is 150 by 100 μm^2 , and the total effective optical detectable area is 1000 by 1000 μm^2 . With appropriate calibration, the curvature-optimized device could be applied in the spectrometer.

2.3 Grating Table

The grating (140nm deep, with 5 μm pitch) on the Al alloy shown in Fig. 4 was patterned by an aluminum etchant made of ferricyanide and KOH that does not attack ZnO. The cross section view of the grating was measured by an atomic force microscope (AFM), and the scanning result is shown in the Figure 5. The average roughness of the grating is around 50 nm, a decent number for optical spectrometer application. However, the aluminum etchant will attack the sacrificial layer (photoresist) under a long etching time. Chlorine based plasma would have worked better to etch the aluminum for forming the grating.

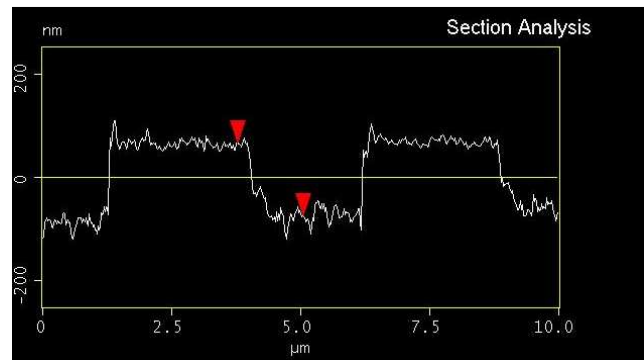


Figure 5: AFM scanning result of the grating on the unreleased aluminum alloy shown in Fig. 1.

3 MEASUREMENT RESULTS

3.1 Mechanical Response

Using laser Doppler vibrometer, we measured the angular displacement of the mirror array as a function of frequency (Fig. 6). With ± 5 V peak-to-peak sinusoidal wave input, the mirror structure was measured to have 0.42 μm

peak-to-peak displacement at its first resonant frequency, which corresponds to $0.025^\circ/\text{V}$, several times lower than expected but adequate for 400 - 700nm range. The first resonant frequency of the mirror supported by the piezoelectric cantilever was around 5.4 kHz, which is around ten times lower than that of a piezoelectric cantilever by itself without the mirror, due to the added mass of the mirror.

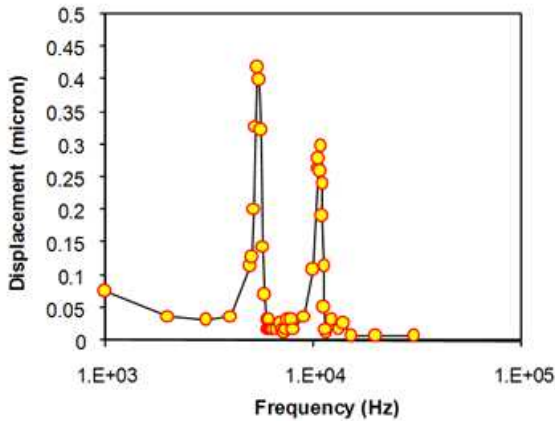


Figure 6: Measured displacement of one mirror.

3.2 Optical Performance

Helium-neon laser (having $0.6328 \mu\text{m}$ wavelength) was used to measure the reflectivities of various structures. First, the sputtered aluminum alloy was measured to have a maximum reflectivity around 90% (Fig. 7), which can be improved by optimizing the sputter deposition process to make the surface smoother. Thinner aluminum alloy or flatter sacrificial layer underneath the alloy also will translate into an increased reflectivity.

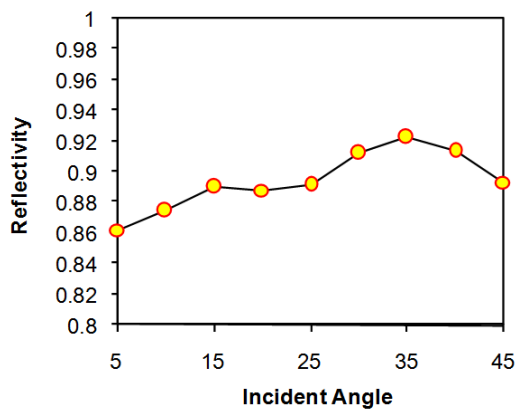


Figure 7: Reflectivity of unpatterned aluminum alloy.

The measured reflectivity of a mirror array before the final XeF_2 etching of the silicon was measured to be around 12% (Fig. 8). The low reflectivity is due to (1) the low fill factor caused by poor photolithography at a university lab

and (2) the array diffraction. By optimizing the individual mirror size and the spacing between the mirrors, the reflectivity can be increased to close to 90%.

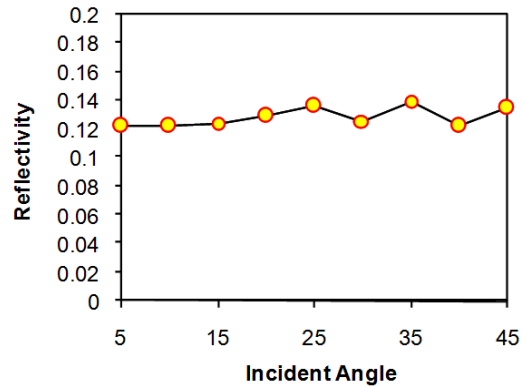


Figure 8: Measured reflectivity of the patterned mirror array.

The fabricated piezoelectric mirror array was applied to the spectrum imaging by aligning the mirror array to a fixed Al grating with pitch of $5 \mu\text{m}$ and grating depth of $0.1 \mu\text{m}$. The diffraction efficiency of the combination was measured for three different diffraction orders (Fig. 9).

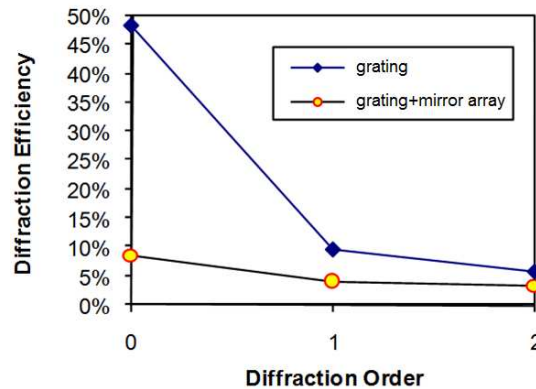


Figure 9: Measured diffraction efficiency of the grating and mirror array with grating.

4 DISCUSSION

Several challenges exist in realizing the actuated micrograting. First of all, long cantilever actuators (needed for the large wavelength separation) result in initial warping due to residual stress and/or stress gradient. The warping stiffens the cantilever, and reduces the amount of the angular displacement per applied voltage. For the same reason, it is difficult to fabricate a large suspended thin plate of $150 \times 100 \mu\text{m}^2$ (for the grating/mirror) without warping, if its three edges are released. Finally, it is difficult to pattern fine grating pitch on the aluminum plate on top of the photoresist sacrificial layer due to the surface roughness caused by the distorted shape around the anchor

of the grating/mirror plane and thick sputtered aluminum alloy.

The optical resolution can be improved by increasing the grating power (i.e. the line density). The scanning range can be improved with polishing of the mirror/grating surface and/or making the cantilever flat through stress compensation of the layers.

5 SUMMARY

The fabricated piezoelectric mirror array was applied to the spectrum imaging by aligning the mirror array to a fixed Al grating with pitch of 5 μm and grating depth of 0.1 μm . The diffraction efficiency of the combination was measured for three different diffraction orders. We also measured the angular displacement of the mirror array as a function of frequency. With ± 5 V peak-to-peak sinusoidal wave input, the mirror structure was measured to have 0.42 μm peak-to-peak displacement at its first resonant frequency, which corresponds to 0.025 $^\circ$ /V. The first resonant frequency of the mirror supported by the piezoelectric cantilever was around 5.4 kHz. Furthermore, we fabricated a piezoelectric grating array, which can be integrated to form a wavelength-selectable, compact 2D spectrometer.

6 ACKNOWLEDGMENT

This material is based on the work supported by NIH Grant NO. R21EB3628. The authors would like to thank Chuang-Yuan Lee and Hongyu Yu for their valuable helps in the fabrication process.

7 REFERENCES

- [1] R. F. Wolffenbuttel, "MEMS-based optical mini- and microspectrometers for visible and infrared spectral range," *JMM*, (15): 145-52, 2005.
- [2] P. C. Montgomery, D. Montaner, O. Manzardo, M. Flury and H. P. Herzig, "The metrology of a miniature FT spectrometer MOEMS device using white light scanning interference microscopy", *Thin Solid Films*, 450, 79-83, 2004.
- [3] E. Shields, W. Zhou, Y. Wang, J. Leger, "Microelectromechanical system-based adaptive space-variant imaging microspectrometer," *Appl Opt.*, 46(31): 7631-9, 2007.
- [4] S. Grabarnik, A. Emadi, E. Sokolova, G. Vdovin, R.F. Wolffenbuttel, "Optimal implementation of a microspectrometer based on a single flat diffraction grating," *Appl Opt.*, 47(12): 2082-90, 2008.
- [5] Jarek Antoszewski, John Dell, Thananjeyan Shivakumar, Mariusz Martyniuk, Kevin Winchester, Justin Wehner, Charlie Musca and Lorenzo Faraone, "Towards MEMS based infrared tunable micro-spectrometers", *Proc. Soc. Photoinst. Opt. Eng.* 4935, 148-155, 2002.
- [6] P. Cheben, J. H. Schmid, A. Del age, A. Densmore, S. Janz, B. Lamontagne, J. Lapointe, E. Post, P. Waldron, and D.-X. Xu, "A high-resolution SOI arrayed waveguide grating microspectrometer with submicrometer aperture waveguides," *Opt.Express*, 15(5): 2299-306, 2007
- [7] J. Lo, S.J. Chen, Q. Fang, T. Papaioannou, E.S. Kim, M. Gundersen, L. Marcu, "Performance of a diaphragmed microlens for a packaged microspectrometer," *Sensors*, 9(2) p859-698, 2009.
- [8] Q. Fang, Papaioannou, T., Jo, J.A., Vaitha, R., Shastry, K., Marcu, L., "Time-domain laser-induced fluorescence spectroscopy apparatus for clinical diagnosis," *Review of Scientific Instruments*, 75(1) p151-162, 2004.
- [9] D.S. Elson, J. Jo, L. Marcu, "Miniaturized side-viewing imaging probe for fluorescence lifetime imaging (FLIM): validation with fluorescence dyes, tissue structural proteins and tissue specimens," *New J. Phys.* 9(127), 2007.
- [10] J. Jo, Q. Fang, T. Papaioannou, L. Marcu, "Laguerre-based method for analysis of time-resolved fluorescence data: application to in-vivo characterization and diagnosis of atherosclerotic lesions," *J. Biomed. Opt.*, 11, 2006.